

Estimation of Specific Absorption Rate Levels in a Typical Fruit Specimen and Observations on their Variations According to Different Electromagnetic Standards

Ardhendu Kundu[#], Bhaskar Gupta, Amirul I. Mallick

Abstract – Estimation of Specific Absorption Rate levels in a typical bunch of Sapodilla fruits is presented. Detailed discussion on their variations, due to the existing disparity among the electromagnetic standards is presented in a quantitative manner. The work includes dielectric properties characterization of the fruit specimen and the modelling of a typical fruit bunch according to their dielectric properties for the simulation-based investigations in order to gauge the Specific Absorption Rate levels based on the exposure standards. A typical geometric shape of the fruit bunch, modelled only under the most practical considerations – is also taken, in order to replicate the exact natural scenario, where the fruits or the other plant tissues are irradiated with electromagnetic exposures from the mobile towers and other Radio Frequency energy sources. The variations in the estimated Specific Absorption Rate levels calculated under different electromagnetic standards prescribed globally are seen to be substantial and the records are presented in detail in this article. Rigorous simulation works are carried out, to ensure accurate comparison between the estimated Specific Absorption Rate levels. Two global and two national electromagnetic standards are taken for the comparisons; both occupational and public exposure standards are considered. Five different frequencies of mobile operations are also considered as possible RF exposure sources in this work, for the investigations. The variation existing between the estimated Specific Absorption Rate levels based on the different standards in each of the frequencies - suggests a critical evaluation of the status quo and calls for the need of maintaining a global homogeneity among the existing Radio Frequency exposure regulations.

Keywords – Biological effects of radiation, Dielectric properties characterization of plant tissues, Electromagnetic regulatory standards, Open ended coaxial probe technique, Specific absorption rate estimation in fruit specimen.

I. INTRODUCTION

Seamless connectivity requirements initiated hard challenges for the telecom service providers, who in turn – have exhaustively used up the available bandwidths, leading

Article history: Received January 01, 2020; Accepted December 13, 2021

Ardhendu Kundu[#] (corresponding author) and Bhaskar Gupta are with the Department of Electronics and Telecommunication Engineering, Jadavpur University, Kolkata, India 700032, E-mails: [#]ardhendukundu.1989@gmail.com, gupta_bh@yahoo.com

Amirul I. Mallick is with the Indian Institute of Science Education and Research Kolkata, India 741246, E-mail: amallick@iiserkol.ac.in

to continuous electromagnetic emission in nature. With the major frequency bands being used for telecom services (like 900 MHz, 1800 MHz, 2100 MHz, 2300 MHz, 2400 MHz, and so on), the present world lives under the shadow of continuous Radio Frequency (RF) signals and exposures today. This electromagnetic energy emitted from the cell tower antennas, gets absorbed in biological masses (be it humans or plants) due to reasonably high dielectric properties of living tissues. The dielectric properties of such tissues and biological masses are extensively studied in the references [1]-[17]. In addition, adequate literature is available regarding the electromagnetic energy deposition in humans [18]-[29] with some recent work on plants and fruits too [30]-[38]. The electromagnetic energy deposition rate (in humans as well plants) is quantitatively measured in terms of Specific Absorption Rate (SAR) and it is defined as the amount of power absorbed in one unit of biological mass while exposed to an external incident electromagnetic field [18]-[38]. At present, several RF exposure guidelines are in effect across the globe to gauge and check the maximum permissible SAR limits in humans for health reasons [39]-[42]. However, no such regulations are there for fruits, crops, or plants in general. In recent times, SAR estimations in several partial plant models such as for fruits, flowers, and other plant parts are being considered [30]-[38] to draw attention of the global authorities in this context.

In addition to the basic SAR limit regulations (for humans), frequency dependent reference electromagnetic field strengths for far field exposures have also been capped at different levels depending upon the regulatory standards in effect, for the concerned geographical regions [39]-[45]. However, no such measures are adopted for plants, crops, or fruits, which too, are at the same time getting exposed to RF radiation in a continuous manner. On the other hand, significant amount of disparity exists among the RF regulatory guidelines, in terms of – the reference electromagnetic power density levels, and the variation lies in the order of as high as ten to hundred folds among the standards [39]-[45]. SAR value depends extensively upon the strength of incident electromagnetic field, in addition to wave polarization, angle of incidence, material properties, and geometrical shapes of biological objects [30]-[38]. Therefore, the existing disparity among different electromagnetic standards plays an important role in determining the electromagnetic energy deposition rates, in terms of SAR values of the objects concerned [37].

Till date, quantitative estimation of electromagnetic energy absorption rate in composite bunch of fruits structure is less frequently reported in literature. In general, different fruits and plants are of different geometrical shapes and they possess dissimilar dielectric properties. Consequently, one unique prototype model is neither sufficient nor exhaustive, to conceive the problem and to investigate the phenomenon of electromagnetic energy absorption in fruits and plants respectively. SAR investigations in single fruit models [30]-[33], bunches of fruits models [34], [38], and multilayer fruit models [35]-[36] have already been reported. However, except for a plant prototype [37], no comparative SAR investigations have been performed in any fruit model based on the existing disparities among different electromagnetic standards. This article therefore, aims at dielectric properties characterization and three dimensional modelling of a typical bunch of sapodilla fruits along with a connected leaf structure, to investigate and observe the contrast in SAR data records with respect to the existing disparities among the different electromagnetic standards. Two global and two national RF exposure standards are taken for the comparisons [39]-[42]; both occupational and public standards are considered. Five different frequencies of mobile operations are also considered as possible RF exposure sources in this work, for the investigations. The results may lead to a future establishment of uniform electromagnetic standards for plants, crops, fruits, and other living objects concerned, after investigating the associated biological effects as well, due to the exposures.

Section II of this article deals with the definition of SAR, and a comparative discussion on the permissible electromagnetic exposure limits as established by the global and national standards. This is followed by a detailed discussion on the dielectric properties characterization of biological tissues and their material properties in Section III. The simulation process is detailed in Section IV. Collective results along with detailed discussions are presented in Section V followed by the conclusions and a list of references.

II. DEFINITION OF SPECIFIC ABSORPTION RATE AND DISPARITY AMONG GLOBAL AND NATIONAL ELECTROMAGNETIC STANDARDS

Electromagnetic energy absorption rate in biological mass is quantified in terms of SAR that is further categorized as maximum local point SAR (MLP SAR), SAR averaged over 1g of contiguous mass (1g SAR), SAR averaged over 10g of contiguous mass (10g SAR), and SAR averaged over the entire biological mass (WBA SAR). SAR at a particular point is defined by the following mathematical relation illustrated in Eq. (1):

$$SAR = \frac{\sigma|E|^2}{\rho}, \quad (1)$$

where, σ is electrical conductivity of biological tissue, E is electric field (r.m.s) strength developed inside biological tissue, and ρ is material density of biological tissue. Moreover, 1g SAR, 10g SAR, and WBA SAR are basically

TABLE I
DISPARITY AMONG DIFFERENT GLOBAL AND NATIONAL ELECTROMAGNETIC GUIDELINES [39]-[45]

Frequency of exposure (MHz)	Prescribed power density level (W/m ²)					
	Occupational Zone		Public Zone			
	FCC	ICNIRP	FCC	ICNIRP	India	Swiss
947.5	31.58	23.69	6.32	4.74	0.47	0.047
1842.5	50	46.06	10	9.21	0.92	0.092
2150	50	50	10	10	1	0.1
2350	50	50	10	10	1	0.1
2450	50	50	10	10	1	0.1

averages of local point SAR data over respective contiguous tissue masses. SAR value depends upon square of electric field strength magnitude developed, tissue conductivity, tissue density, geometrical shape, frequency of irradiation, wave polarization, and angle of wave incidence etc [18]-[38].

As described in Eq. (1), the electromagnetic energy absorption rate varies with square of the internal electric field strength magnitude developed. Furthermore, the internal electric field strength magnitude develops in direct proportion with the incident electric field strength on the object. Hence, disparity among different global and national electromagnetic standards plays an important role while investigating SAR distribution in a specific biological object at a particular frequency of irradiation. Global electromagnetic standards prescribed by the organizations like Federal Communications Commission (FCC) and International Commission on Non-Ionizing Radiation Protection (ICNIRP) are adopted over a considerable part of the world to defend possible health risks [39]-[40]. But, reference power density levels (below 2000 MHz) for public exposure prescribed by these two organizations don't precisely agree with each other. Research outcomes on electromagnetic energy absorption rate in human phantoms along with consequent biological responses have raised concerns among the scientists and general public as well [18]-[29], [46]-[53]. In response, competent authorities in nations like Switzerland and India etc. have prescribed stricter national electromagnetic standards [41]-[42]. However, these global and national electromagnetic standards are not at par in terms of reference power density levels – with variations ranging from ten to hundred folds (refer to Table I) [39]-[45].

III. DENSITY AND DIELECTRIC PROPERTIES CHARACTERIZATION OF SAPODILLA FRUIT, LEAF, AND TWIG SPECIMENS

Adequate numbers of fresh sapodilla fruits along with connected leaves have been taken to laboratory for material density measurement and dielectric properties characterization. Thereafter, half of the samples have been taken for material density measurement and rest have been used in dielectric characterization technique.

A. Material Density Characterization

For material density characterization, mass of individual sapodilla fruit, leaf, and twig specimen has been weighed using scientific balance. Volume of individual specimen has been measured. Thereafter, material densities of sapodilla fruit, leaf, and twig specimens have been calculated. Obtained data have been averaged over similar specimens and illustrated in Table II.

B. Dielectric Properties Characterization

A number of established techniques like open ended coaxial probe, transmission line method, free space method, resonant cavity method, parallel plate method, planar transmission line method etc. are utilized for dielectric properties characterization [54]-[56]. However, each technique has its own advantages and drawbacks. Appropriate measurement techniques therefore should be adopted depending upon the physical state and approximate dielectric parameter range of the material under test. Open ended coaxial probe technique is considered to be the most suitable for broadband dielectric properties characterization of lossy biological samples that are semi-solid or liquid in nature (or at least contain reasonably high amount of liquid) [2]-[5], [16]-[17], [30]-[38], [57]-[62]. Theoretical analysis of open ended coaxial probe technique for broadband dielectric properties measurement is well established in literature [2]-[5], [35], [57]-[60]. In this context, mathematical analysis of antenna impedance in conducting medium was reported by Deschamps way back in 1962 [57]. In between 1980 to 1982, Stuchly et al. reviewed and demonstrated open ended coaxial probe technique for dielectric properties characterization of several biological samples at microwave frequencies [2]-[4]. In brief, equivalent circuit model for open ended coaxial probe contains a parallel combination of the fringing capacitance from inner to outer conductor through material under test, another fringing capacitance from the inner to outer conductor via intervening material (Teflon in most cases) within the coaxial probe, along with a radiation conductance representing propagation loss through material under test. For an open ended coaxial probe with known dimensions, effective values of two parallel

TABLE II
MEASURED MATERIAL DENSITY (ρ) OF SAPODILLA FRUIT,
LEAF, AND TWIG SAMPLES

Name of sample	Sapodilla	Leaf	Twig
Material density (kg/m ³)	1107.8	833.3	1107.8

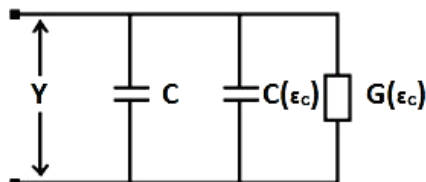


Fig. 1. Analytical model of an open ended coaxial probe in lossy medium [2], [35], [58]-[60].

capacitances and conductance depend on the frequency of operation along with the complex dielectric properties of the material under test. Fig. 1 illustrates an equivalent circuit model of open ended coaxial probe [2], [35], [58]-[60].

The input admittance of open ended coaxial probe can be expressed as follows in Eq. (2) [2], [35], [58]-[60]. Eq. (2a) and Eq. (2b) are modified for air/vacuum and deionized water respectively.

$$Y = G(\epsilon_c, \omega) + j\omega C(\epsilon_c, \omega), \quad (2)$$

$$Y_0 = G_0(1, \omega) + j\omega C_0(1, \omega), \quad (2a)$$

$$Y_w = G_w(\epsilon_w, \omega) + j\omega C_w(\epsilon_w, \omega), \quad (2b)$$

where, G_0 and G_w are conductance values while the probe is in air/vacuum and deionized water respectively. C_0 and C_w are capacitances while the probe is in air/vacuum and deionized water. ϵ_c and ϵ_w are complex relative permittivity of biological sample and deionized water; whereas, ω is the frequency of operation.

In case of biological tissue medium beneath the open ended coaxial probe, the same is analytically modelled as an antenna in lossy medium (Deschamps's theorem, 1962) as illustrated in Eq. (3) and Eq. (4) respectively [57]-[60]. Eq. (4a) is the modified version of Eq. (4) in deionized water for system calibration and error minimization.

$$Y(\epsilon_c, \omega) = \sqrt{\epsilon_c} Y_0(1, \omega \sqrt{\epsilon_c}), \quad (3)$$

$$Y = j\omega \epsilon_c C_0 + \sqrt{\epsilon_c} G_0, \quad (4)$$

$$Y_w = j\omega \epsilon_w C_0 + \sqrt{\epsilon_w} G_0, \quad (4a)$$

Capacitance C_0 is considered to have negligible variation in free space; capacitance C_0 and radiation conductance G_0 are calculated using Eq. (4) and Eq. (4a) derived by Liu et al. while the antenna (open ended coaxial probe) is in air/vacuum and deionized water respectively [58].

Open ended coaxial probe is calibrated using the following technique. First, a complex input admittance data set is calculated from measured reflection coefficient data set (S_{11}) using Vector Network Analyzer (VNA) for standard references with known dielectric parameters (air and deionized water at 25°C); choosing deionized water as the standard reference during calibration also facilitates accurate characterization of biological tissues that possess reasonable amount of water content resulting in high permittivity. Complex input admittance data of open ended coaxial probe are calculated from measured reflection coefficient data (S_{11}) using the following relation illustrated in Eq. (5) [35], [60]:

$$Y = Y_0 \left[\frac{1-S_{11}}{1+S_{11}} \right], \quad (5)$$

where, $Y_0 = \frac{1}{50 \Omega} = 0.02 S$; (Y_0 is characteristics admittance of open ended coaxial probe).

Then, the calculated complex input admittance data and the complex dielectric properties of reference materials are

processed to find out radiation conductance G_0 and fringing capacitance C_0 of open ended coaxial probe in air. Finally, the derived radiation conductance G_0 and the fringing capacitance C_0 are used further to characterize dielectric properties of the unknown material under test [35], [60].

Coming to the practical dielectric measurement setup, dielectric properties i.e. real part of complex permittivity (ϵ_r) and loss tangent ($\tan \delta$) data for sapodilla fruit, leaf, and twig specimens have been characterized using 85070E open ended coaxial probe dielectric measurement kit (Agilent Technologies) along with E5071B ENA Series VNA (Agilent Technologies). Figs. 2(a), 2(b), and 2(c) illustrate dielectric properties measurement set up for sapodilla fruit and leaf specimens using above mentioned open ended coaxial probe technique. The open ended coaxial dielectric measurement kit contains a high temperature coaxial probe that can withstand up to 200°C and can measure dielectric properties maximum up to 20 GHz. But, dielectric properties have been measured up to 8.5 GHz due to the frequency limitation of E5071B ENA Series VNA (Agilent Technologies). As a consequence, dielectric properties for sapodilla fruit and leaf specimens have been characterized up to 8.5 GHz. During dielectric properties characterization, adequate numbers of sapodilla leaves have been stacked to ensure negligible contribution from the base material beneath stacked leaves on measured reflection coefficient data at open ended coaxial probe interface. Thickness of stacked sapodilla leaves has been ensured more than twice the skin depth to ascertain accurate dielectric properties measurement. Dielectric properties for sapodilla twig couldn't be characterized separately due to small diameter of the twigs compared to diameter of the open ended coaxial probe (2 cm) – thus, the twig has been considered to possess similar dielectric properties to that of sapodilla leaves. Measured dielectric properties of sapodilla fruit, leaf, and twig (considered) samples have been tabulated in Table III.

IV. DESIGN OF A TYPICAL SAPODILLA BUNCH PHANTOM AND SAR SIMULATION SETUP

A. Design of a Typical Sapodilla Bunch Phantom in CST Microwave Studio

A typical three dimensional bunch of sapodilla fruits along with a leaf has been prototyped in CST Microwave Studio 2014 [63]. The bunch containing three fruits is weighing 121.16 g and occupying a volume of 109.58 cm³. Three

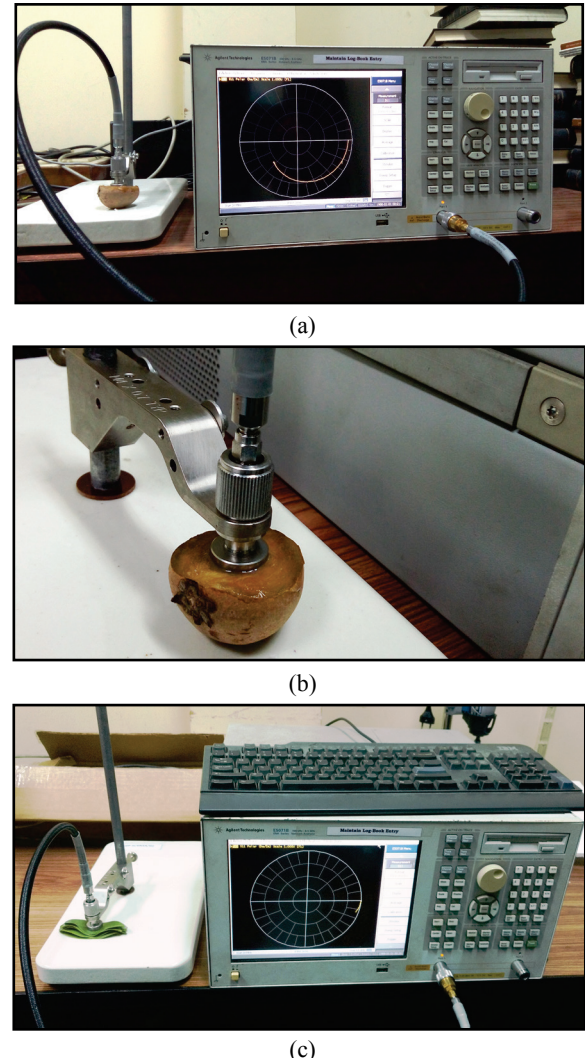


Fig. 2. Broadband permittivity and loss tangent measurement setup using Agilent 85070E dielectric measurement kit and E5071B ENA series Vector Network Analyzer (VNA) (a) Sapodilla fruit, (b) Enlarged view of open ended coaxial probe on flat cut surface of sapodilla fruit, and (c) Sapodilla leaves.

sapodilla fruit specimens have been designed as spheres of different radii. A typical medium sized leaf has been first outlined on graph paper – then two dimensional coordinates have been imported and extruded to replicate the three dimensional leaf with specified thickness. The finalized prototype of three dimensional bunch of sapodilla fruits phantom has been illustrated in Fig. 3. In addition, exact geometrical specifications of the developed model are listed in Table IV.

TABLE III
MEASURED PERMITTIVITY AND LOSS TANGENT OF SAPODILLA FRUIT, LEAF, AND TWIG SAMPLES

Sample	947.50 MHz		1842.50 MHz		2150 MHz		2350 MHz		2450 MHz	
	ϵ_r	$\tan \delta$								
Fruit	66.08	0.222	64.33	0.217	63.30	0.237	62.67	0.239	62.90	0.248
Leaf	33.21	0.438	30.33	0.358	29.72	0.348	29.26	0.358	29.32	0.350
Twig	33.21	0.438	30.33	0.358	29.72	0.348	29.26	0.358	29.32	0.350

B. SAR Simulation with Linearly Polarized Plane Wave Incidence

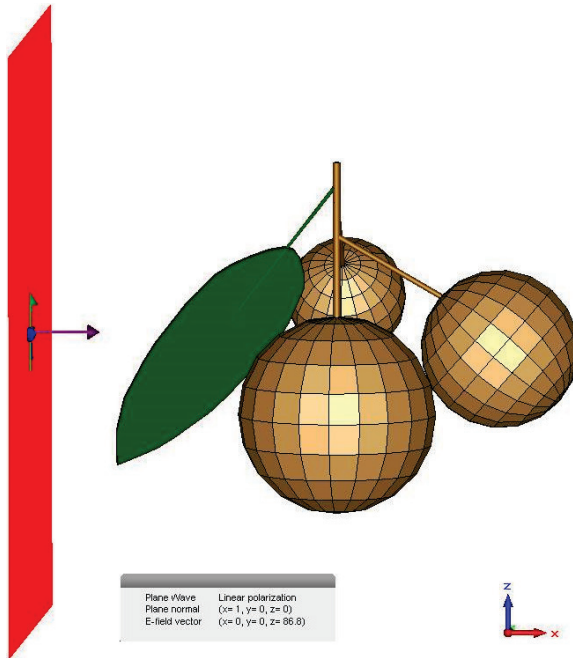


Fig. 3. Three dimensional CAD model of the bunch of sapodilla fruits with linearly polarized plane wave at 1842.50 MHz in accordance with FCC public exposure scenario.

TABLE IV
MODELLING SPECIFICATIONS OF BUNCH OF SAPODILLA FRUITS

Fruit Sample Specifications				
Sapodilla fruit	Shape	Radius (mm)		
Large	spherical	25		
Medium	spherical	20		
Small	spherical	15		
Leaf Sample Specifications				
Leaf	Shape	Length (mm)	Width (mm)	Thickness (mm)
Leaf blade	Thin planner	80	30	0.5
Twig Sample Specifications				
Twig	Shape	Length (mm)	Radius (mm)	
Primary twig connected to large fruit	cylindrical	40	1	
Secondary twig connected to medium fruit	cylindrical	30	0.7	
Secondary twig connected to small fruit	cylindrical	25	0.7	
Secondary twig connected to leaf blade	cylindrical	20	0.5	

The bunch of sapodilla fruits specimen is irradiated with plane waves as per the contrasting global and nationalized electromagnetic standards. Linearly polarized plane waves with different electric field strengths, depending upon the frequency of exposure and regulatory standards in effect, have been used as far-field radiation sources. CST Microwave Studio 2014 simulator accounts peak electric field strength as an input for linearly polarized plane wave set up [63]. Hence, prescribed unperturbed r. m. s. electric field strength has been multiplied each time by $\sqrt{2}$ to obtain the peak electric field strength (considering sinusoidal variation) [39]-[42]. The transient solver available in CST Microwave Studio 2014 has been utilized to estimate the SAR values for the prototyped bunch of sapodilla fruits [63]. Total number of mesh cells in the above mentioned prototyped specimen is about 0.25 million in number with an average mesh cell size of 0.004 g. Four Perfectly Matched Layers (PMLs) with 10^{-4} reflection coefficient have been used as electromagnetic absorbing boundaries during simulation. Distance between the bunch of sapodilla fruits and the boundary wall has been kept negligible by choosing appropriate boundary conditions. Maximum local point SAR, 1g averaged SAR, 10g averaged SAR, and whole body averaged SAR data are compared in accordance with the above mentioned electromagnetic standards [39]-[42]. SAR data (except point SAR data that don't require averaging) have been averaged using three standard protocols, viz. IEEE C95.3 [64], CST C95.3 [63], and the most recent IEEE/IEC 62704-1 [65] SAR averaging techniques. However, insignificant variations are noted among the obtained datasets while three different SAR averaging protocols have been adopted. Hence, all SAR data have been reported adopting the most recent IEEE/IEC 62704-1 SAR averaging protocol only [65].

V. COMPARATIVE SAR DATA AND ANALYSIS

A. SAR Simulation Results

SAR data have been simulated mimicking occupational as well as public global exposure scenarios [39]-[40]. Moreover, SAR simulations have also been performed in accordance with selected nationalized public exposure scenarios in countries like India and Switzerland [41]-[42]. SAR data have been estimated at 947.5 MHz, 1842.5 MHz, 2150 MHz, 2350 MHz, and 2450 MHz respectively. Earlier, Fig. 3 showed a typical linearly polarized plane wave impinging on the bunch of sapodilla fruits specimen at 1842.5 MHz as per FCC public exposure standards [39]. Consequent MLP SAR and 1g averaged SAR distributions have been illustrated in Figs. 4(a) and 4(b) respectively [39]. The contrasts obtained in the comparative SAR datasets for the bunch of sapodilla fruits at five different frequency bands have been summarized over Table V to Table IX in sequence with the illustrations in Figs. 5(a) to 5(e). Fig. 5(f) depicts the contrast in cumulative SAR data over all the five frequencies for the above mentioned bunch of sapodilla prototype.

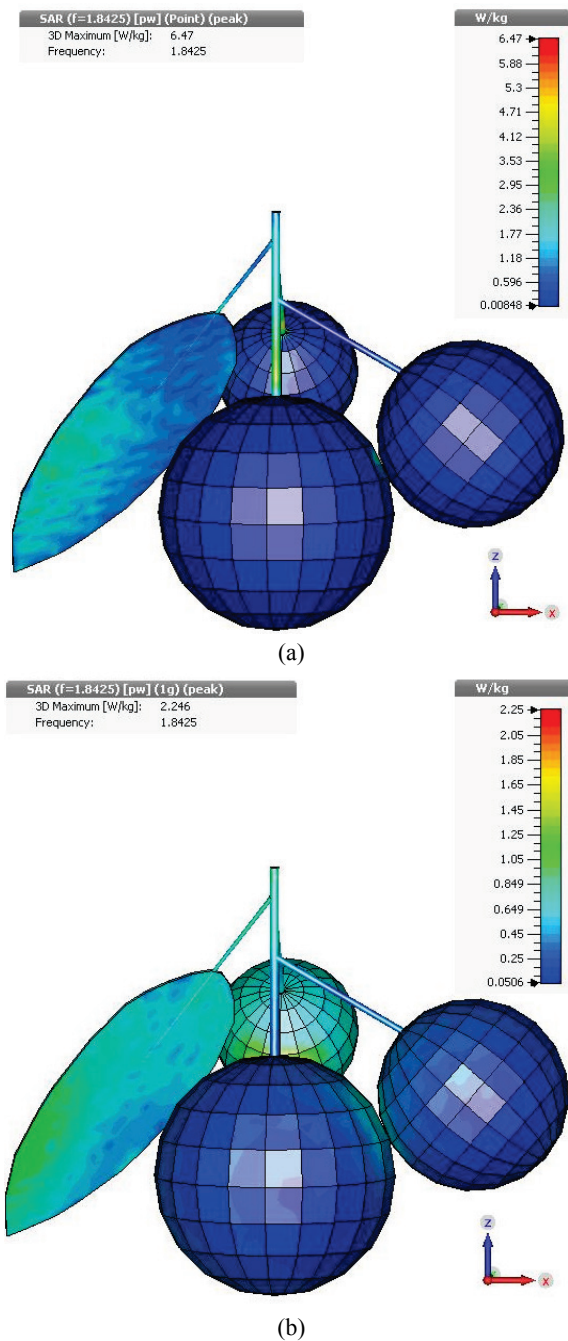


Fig. 4. (a) Simulated point SAR profile on surface of sapodilla bunch at 1842.50 MHz in accordance with FCC public exposure scenario and (b) Simulated 1g averaged SAR profile on surface of sapodilla bunch at 1842.50 MHz in accordance with FCC public exposure scenario.

B. Result Analysis

It is observed in Figs. 4(a) and 4(b) that SAR distribution increases near the surface with sharp geometries i.e. a surface with higher curvature or smaller radius. Charge density at the locations of greater surface curvature tends to be greater in magnitude. This could also be proved by solving the Poisson's equation on and around the surface of arbitrary shapes [66].

Local electric field due to such non uniform charge densities tends to follow a similar pattern i.e. the electric field near a location with greater charge density is also greater in magnitude [67]. The phenomena of increased electric field concentration near the sharp edges are not limited to conducting bodies alone [68]. Even in case of a dielectric body with finite conductivity, similar principle applies. Solution of the scattering problem depicted by the scattering of incident electromagnetic field by the said dielectric object eventually leads to an electric field distribution (or an equivalent induced surface current density) that prefers the sharp edges i.e. the magnitude of the distribution is greater near the regions of greater surface curvature.

Reported data reveal that the SAR value in general increases with frequency of exposure in accordance with any particular electromagnetic standards [39]-[42]. It is so because of the following reasons. First of all, the permissible electromagnetic field strength increases with frequency of exposure up to 2000 MHz in most cases (exception: 1500 MHz in case of the FCC electromagnetic standards) and as a consequence of the same, electric field values inside the bunch of sapodilla specimen also increase along with the resultant SAR values [30]-[38]. Hence, a prominent increment in SAR data is observed in between 947.5 MHz to 1842.5 MHz. Moreover, the operating wavelength inside the bunch of sapodilla model shortens with an increase in frequency – resulting in more number of hotspots with intense electric field strengths contributing to increased SAR value [30-38]. In addition, dielectric properties of the sapodilla fruit, leaf, and twig change with frequency i.e. permittivity (ϵ_r) to some extent reduces with frequency but loss tangent ($\tan \delta$) increases to a greater extent with frequency above a crucial point in between 1500 MHz to 2500 MHz for plant tissues in general. As a consequence, SAR value also increases with frequency because of the direct and greater dependence of itself on tissue conductivity (σ) / loss tangent ($\tan \delta$) value. Reported SAR data (be it MLP SAR, 1g SAR, 10g SAR, or WBA SAR) are absolutely justified in terms of averaging duration (six or thirty minutes for public exposure [39]-[42]) – because, plants and fruits are stationary in nature and get exposed to electromagnetic energy throughout their lifespan.

Looking from a different aspect, contrasting SAR data have been noted even at a particular frequency because of disparity among the different electromagnetic standards [39]-[42] (refer to Table V to Table IX along with Figs. 5(a) to 5(e)). It should be noted that two reported occupational electromagnetic standards differ by a slight margin below 2000 MHz and match exactly beyond. Both FCC as well as ICNIRP have set down the occupational electromagnetic standards, five folds tolerant compared to the respective public electromagnetic standards [39]-[40]. SAR ($= \sigma|E|^2/\rho$), being directly dependent upon the square of internal electric field strength magnitude developed inside biological medium i.e. bunch of sapodilla model in this case, varies with the square of incident electric field magnitude / directly with power density of plane wave depending upon electromagnetic standards in effect. In the results, SAR values for the bunch of sapodilla fruits model in the occupational exposure zone are too high in accordance with either FCC or ICNIRP occupational exposure standards.

TABLE V
DISPARITY AMONG SAR DATA FOR BUNCH OF SAPODILLA MODEL AT 947.5 MHZ AS PER DIFFERENT GLOBAL AND NATIONALIZED ELECTROMAGNETIC STANDARDS

Frequency 947.5 MHz						
Exposure Zone	Occupational			Public		
Guidelines	FCC	ICNIRP	FCC	ICNIRP	India	Swiss
Power density (W/m²)	31.58	23.69	6.32	4.74	0.47	0.047
Equivalent peak electric field (V/m)	154.3	133.6	69.02	59.77	18.82	5.95
MLP SAR	29.82	22.45	5.96	4.49	0.45	0.045
1g SAR	4.92	3.67	0.98	0.73	0.07	0.007
10g SAR	2.79	2.11	0.56	0.42	0.04	0.004
WBA SAR	1.44	1.08	0.29	0.22	0.02	0.002

SAR is in W/kg

TABLE VII
DISPARITY AMONG SAR DATA FOR BUNCH OF SAPODILLA MODEL AT 2150 MHZ AS PER DIFFERENT GLOBAL AND NATIONALIZED ELECTROMAGNETIC STANDARDS

Frequency 2150 MHz						
Exposure Zone	Occupational			Public		
Guidelines	FCC	ICNIRP	FCC	ICNIRP	India	Swiss
Power density (W/m²)	50	50	10	10	1	0.1
Equivalent peak electric field (V/m)	194.14	194.14	86.82	86.82	27.45	8.68
MLP SAR	39.91	39.91	7.98	7.98	0.80	0.08
1g SAR	10.50	10.50	2.10	2.10	0.21	0.021
10g SAR	4.78	4.78	0.96	0.96	0.10	0.01
WBA SAR	2.07	2.07	0.41	0.41	0.04	0.004

SAR is in W/kg

TABLE VI
DISPARITY AMONG SAR DATA FOR BUNCH OF SAPODILLA MODEL AT 1842.5 MHZ AS PER DIFFERENT GLOBAL AND NATIONALIZED ELECTROMAGNETIC STANDARDS

Frequency 1842.5 MHz						
Exposure Zone	Occupational			Public		
Guidelines	FCC	ICNIRP	FCC	ICNIRP	India	Swiss
Power density (W/m²)	50	46.06	10	9.21	0.92	0.092
Equivalent peak electric field (V/m)	194.14	186.33	86.82	83.33	26.35	8.33
MLP SAR	32.35	29.80	6.47	5.96	0.60	0.060
1g SAR	11.23	10.35	2.25	2.07	0.21	0.021
10g SAR	4.60	4.23	0.92	0.85	0.08	0.008
WBA SAR	2.06	1.90	0.41	0.38	0.04	0.004

SAR is in W/kg

From Table V and Table VI, it is observed that power density levels prescribed in FCC occupational standards (compared to ICNIRP) are 33 percent and 8.5 percent higher at 947.5 MHz and 1842.5 MHz correspondingly. As a consequence, SAR datasets as per FCC standards also differ by respective folds compared to ICNIRP standards; it is so because both incident power density and resultant SAR datasets are related to the second order of electric field strength magnitude at their respective points of observation. Even in case of public exposure, FCC and ICNIRP prescribed power density levels differ by same folds at 947.5 MHz and 1842.5 MHz along with the resultant SAR values (refer to Table V and Table VI along with Figs. 5(a) and 5(b) in order). Nationalized public electromagnetic standards in India and Switzerland are ten to

TABLE VIII
DISPARITY AMONG SAR DATA FOR BUNCH OF SAPODILLA MODEL AT 2350 MHZ AS PER DIFFERENT GLOBAL AND NATIONALIZED ELECTROMAGNETIC STANDARDS

Frequency 2350 MHz						
Exposure Zone	Occupational			Public		
Guidelines	FCC	ICNIRP	FCC	ICNIRP	India	Swiss
Power density (W/m²)	50	50	10	10	1	0.1
Equivalent peak electric field (V/m)	194.14	194.14	86.82	86.82	27.45	8.68
MLP SAR	35.85	35.85	7.17	7.17	0.72	0.072
1g SAR	10.34	10.34	2.07	2.07	0.21	0.021
10g SAR	4.70	4.70	0.94	0.94	0.09	0.009
WBA SAR	1.99	1.99	0.40	0.40	0.04	0.004

SAR is in W/kg

hundred folds stricter compared to the global electromagnetic standards [41]-[42]. As a consequence, SAR values in India and Switzerland are respectively ten to hundred folds lower compared to international standards for public exposure (illustrated in Table V to Table IX). Figs. 5(a) to 5(e) summarize the significant contrast in MLP SAR, 1g SAR, 10g SAR, and WBA SAR values as per different electromagnetic standards over 947.5 MHz to 2450 MHz respectively. SAR values are significantly high where FCC or ICNIRP guidelines are in effect; SAR values are moderate in Indian public exposure scenario but strictly less in Swiss public electromagnetic exposure scenario. However, it must be noted that the safe SAR limit for representative sapodilla plant or any other plant is yet unknown. Moreover, simultaneous

TABLE IX

DISPARITY AMONG SAR DATA FOR BUNCH OF SAPODILLA MODEL AT 2450 MHZ AS PER DIFFERENT GLOBAL AND NATIONALIZED ELECTROMAGNETIC STANDARDS

Exposure Zone	Frequency 2450 MHz					
	Occupational		Public			
Guidelines	FCC	ICNIRP	FCC	ICNIRP	India	Swiss
Power density (W/m^2)	50	50	10	10	1	0.1
Equivalent peak electric field (V/m)	194.14	194.14	86.82	86.82	27.45	8.68
MLP SAR	38.91	38.91	7.78	7.78	0.78	0.078
1g SAR	11.46	11.46	2.29	2.29	0.23	0.023
10g SAR	4.63	4.63	0.93	0.93	0.09	0.009
WBA SAR	1.96	1.96	0.39	0.39	0.04	0.004

SAR is in W/kg

wireless communications in different frequency bands result in cumulative SAR effects i.e. electromagnetic energy absorption in biological tissue adds up over multiple frequencies of wireless communication as illustrated in fig. 5(f). Cumulative SAR data for bunch of sapodilla model over all five frequency bands indicate significant disparity among the different global and nationalized electromagnetic standards and seek immediate attention for uniform electromagnetic standards across the globe.

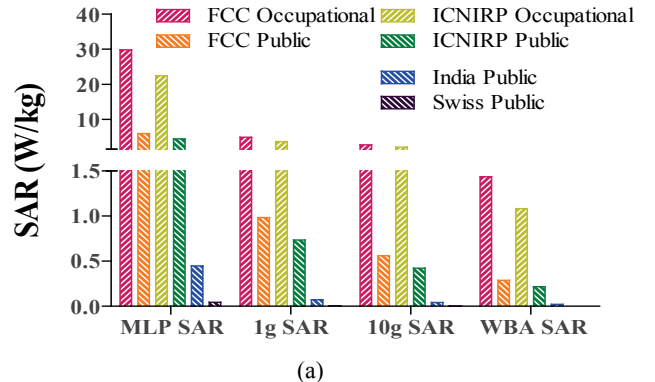
VI. CONCLUSION

SAR data for the prototyped bunch of sapodilla specimen (at a particular frequency) is predominantly dependent on the reference power density prescribed in the electromagnetic standards in effect. SAR datasets in the occupational zone are quite noticeable as FCC and ICNIRP declare occupational premises based on restricted accessibility to public but not based on the presence of plants [39]-[40]. Even more, SAR data at public premises have been noted to be varying by ten to hundred folds depending upon the electromagnetic standards in effect [39]-[42]. SAR data according to the Indian standards have been found to be moderate whereas the same is significantly less in Swiss territory. On contrary, corresponding SAR data in accordance with the global public standards (i.e. FCC and ICNIRP) are quite high and need to be considered with utmost care. Noted disparity among the SAR datasets in accordance with the different electromagnetic guidelines is no different for other biological objects including plants.

Reported SAR data are due to linearly polarized plane wave (direction of propagation along x-axis and electric field along z-axis as illustrated in Fig. 3) that impinges from a specific side of the bunch of sapodilla model. It must be noted that the prototyped bunch of sapodilla specimen is asymmetrical in

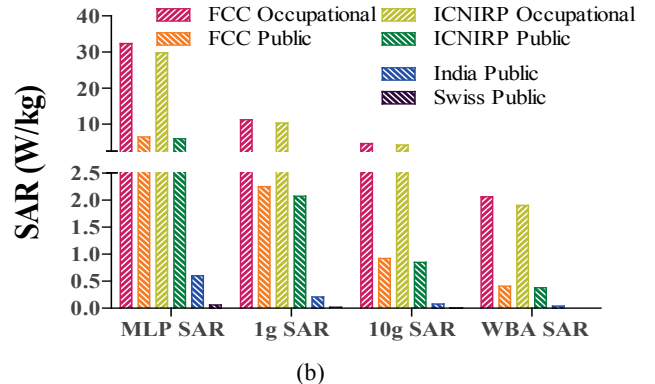
nature and SAR is highly dependent on geometrical shape of the biological object along with direction and polarization of incident wave [36], [38]. Therefore, absolute value of SAR data can differ in case of different plane wave incidence and polarization; however, ratio of SAR values due to the disparity among the different global and nationalized electromagnetic protocols will remain the same in those cases.

Linearly Polarized Plane Wave Exposure at 947.5 MHz



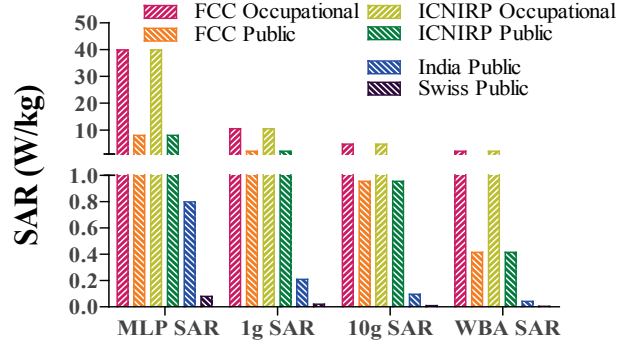
(a)

Linearly Polarized Plane Wave Exposure at 1842.5 MHz



(b)

Linearly Polarized Plane Wave Exposure at 2150 MHz



(c)

Fig. 5. Continued

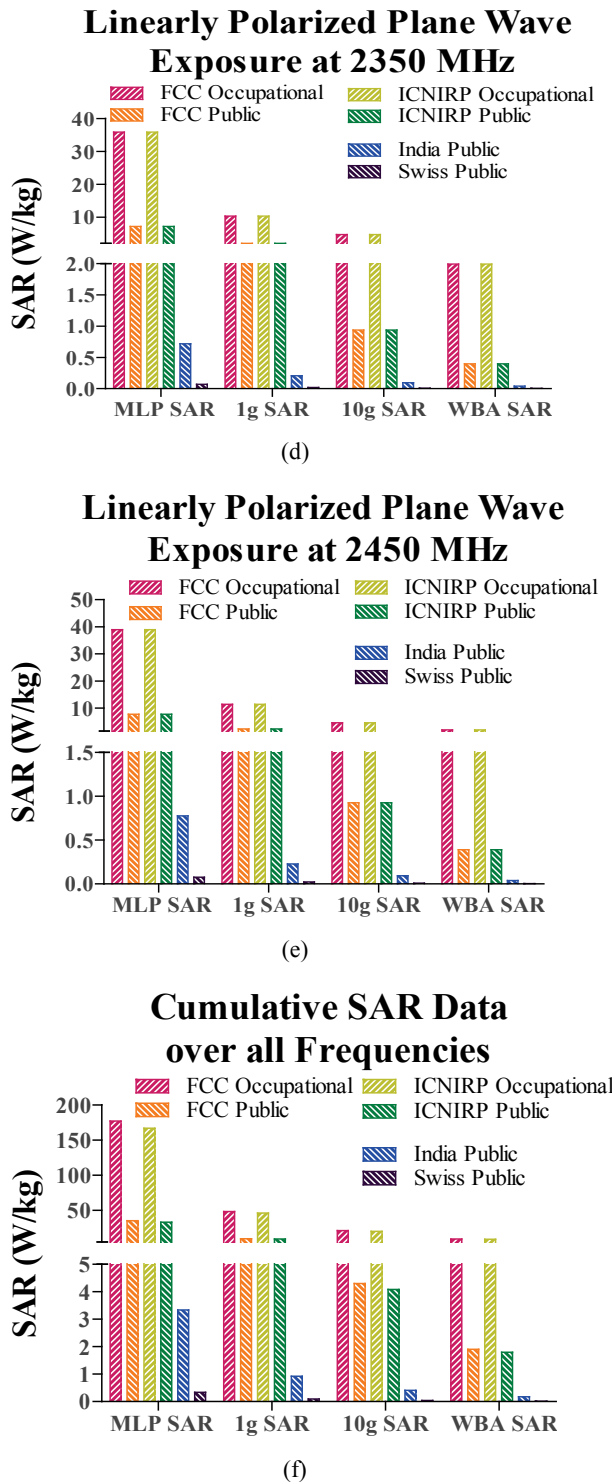


Fig. 5. Disparity among SAR data for the bunch of sаподилла model due to variation among different electromagnetic guidelines (a) Plane wave exposure at 947.5 MHz, (b) Plane wave exposure at 1842.5 MHz, (c) Plane wave exposure at 2150 MHz, (d) Plane wave exposure at 2350 MHz, (e) Plane wave exposure at 2450 MHz, and (f) Cumulative SAR data over all five frequencies mentioned above.

At present, simulated SAR data have been reported and couldn't be extended to practical measurements due to the following reasons. Sapodilla leaf and twig are very thin and

precise electric field measurement inside phantom model is difficult due to significant field perturbation using near field probe. In addition, customized non-standard sapodilla phantom model needs to be imported and same would be quite cost involving. However, work is in progress to develop an indigenous SAR measurement system along with custom made phantom liquid for sapodilla. Hence, simulated SAR data can be considered for the time being and can be backed by practical measurements in future.

Absence of global or local SAR limit for plants makes the situation complicated to scientifically consider an exposure scenario suitable for sustainable plant growth. Therefore, the biological effects of electromagnetic radiation are needed to be studied over a number of plants and fruits [69]-[75]. These investigations can further lead to a subsequent uniform electromagnetic standards implementation worldwide along with the explicit SAR limit prescription for plants and the other biological masses concerned.

ACKNOWLEDGEMENT

This study was funded by Rashtriya Uchchatar Shiksha Abhiyan 2.0 scheme (Govt. of India) at Jadavpur University, India with internal project sanction ref. no. R-11/269/19.

REFERENCES

- [1] H. P. Schwan, "Alternating Current Spectroscopy of Biological Substances", *Proceedings of the IRE*, vol. 7, no. 11, pp. 1841-1855, 1959.
- [2] M. A. Stuchly and S. S. Stuchly, "Coaxial Line Reflection Methods for Measuring Dielectric Properties of Biological Substances at Radio and Microwave Frequencies – A Review", *IEEE Transactions on Instrumentation and Measurement*, vol. 29, no. 3, pp. 176-183, 1980.
- [3] T. W. Athey, M. A. Stuchly and S. S. Stuchly, "Measurement of Radio Frequency Permittivity of Biological Tissues with an Open-Ended Coaxial Line: Part I", *IEEE Transactions on Microwave Theory and Techniques*, vol. 30, no. 1, pp. 82-86, 1982.
- [4] M. A. Stuchly, T. W. Athey, G. M. Samaras and G. E. Taylor, "Measurement of Radio Frequency Permittivity of Biological Tissues with an Open-Ended Coaxial Line: Part II-Experimental Results", *IEEE Transactions on Microwave Theory and Techniques*, vol. 30, no. 1, pp. 87-92, 1982.
- [5] D. Xu, L. Liu and Z. Jiang, "Measurement of the Dielectric Properties of Biological Substances Using an Improved Open-Ended Coaxial Line Resonator Method", *IEEE Transactions on Microwave Theory and Techniques*, vol. 35, no. 12, pp. 1424-1428, 1987.
- [6] C. Gabriel, S. Gabriel and E. Corthout, "The Dielectric Properties of Biological Tissues: I. Literature Survey", *Physics in Medicine & Biology*, vol. 41, no. 11, pp. 2231-2249, 1996.
- [7] S. Gabriel, R. W. Lau and C. Gabriel, "The Dielectric Properties of Biological Tissues: II. Measurements in the Frequency Range 10 Hz To 20 GHz", *Physics in Medicine & Biology*, vol. 41, no. 11, pp. 2251-2269, 1996.
- [8] S. Gabriel, R. W. Lau and C. Gabriel, "The Dielectric Properties of Biological Tissues: III. Parametric Models for the Dielectric Spectrum of Tissues", *Physics in Medicine & Biology*, vol. 41, no. 11, pp. 2271-2293, 1996.

- [9] A. W. Kraszewski, S. Trabelsi and S. O. Nelson, "Broadband Microwave Wheat Permittivity Measurement in Free Space", *Journal of Microwave Power & Electromagnetic Energy*, vol. 37, no. 1, pp. 41-54, 2002.
- [10] S. O. Nelson, "Measuring Dielectric Properties of Fresh Fruits and Vegetables", *IEEE Antennas and Propagation Society International Symposium 2003, Digest. Held in conjunction with: USNC/CNC/URSI North American Radio Sci. Meeting (Cat. No. 03CH37450)*, vol. 4, pp. 46-49, Columbus, Ohio, 2003.
- [11] S. O. Nelson, "Dielectric Spectroscopy of Fresh Fruits and Vegetables", *2005 IEEE Instrumentation and Measurement Technology Conference (IMTC 2005)*, vol. 1, pp. 360-364, Ontario, Canada, 2005.
- [12] S. O. Nelson, S. Trabelsi and S. J. Kays, "Correlating Dielectric Properties of Melons with Quality", *IEEE Antennas and Propagation Society International Symposium 2006*, pp. 4849-4852, USA, 2006.
- [13] W. Guo, S. O. Nelson, S. Trabelsi and S. J. Kays, "10-1800 MHz Dielectric Properties of Fresh Apples during Storage", *Journal of Food Engineering*, vol. 83, no. 4, pp. 562-569, 2007.
- [14] S. O. Nelson, "Dielectric Properties of Agricultural Products and Some Applications", *Res. Agr. Eng.*, vol. 54, no. 2, pp. 104-112, 2008.
- [15] S. O. Nelson and S. Trabelsi, "Dielectric Spectroscopy Measurements on Fruit, Meat, and Grain", *Transactions of the ASABE, American Society of Agricultural and Biological Engineers*, vol. 51, no. 5, pp. 1829-1834, 2008.
- [16] A. Kundu and B. Gupta, "Broadband Dielectric Properties Measurement of Some Vegetables and Fruits Using Open Ended Coaxial Probe Technique", *2014 International Conference on Control, Instrumentation, Energy and Communication (CIEC)*, pp. 480-484, Kolkata, India, 2014.
- [17] A. Kundu, K. Patra and B. Gupta, "Broadband Dielectric Properties Evaluation of *Catharanthus Roseus* Leaf, Flower and Stem Using Open Ended Coaxial Probe Technique", *Journal of Physical Science*, vol. 18, pp. 62-69, 2014.
- [18] S. S. Stuchly, M. A. Stuchly, A. Kraszewski and G. Hartsgrove, "Energy Deposition in a Model of Man: Frequency Effects", *IEEE Transactions on Biomedical Engineering*, vol. 33, pp. 702-711, 1986.
- [19] K. Meier, V. Hombach, R. Kästle, R. Y. Tay and N. Kuster, "The Dependence of Electromagnetic Energy Absorption upon Human-Head Modelling at 1800 MHz", *IEEE Transactions on Microwave Theory and Techniques*, vol. 45, no. 11, pp. 2058-2062, 1997.
- [20] J. Cooper, B. Marx, J. Buhl and V. Hombach, "Determination of Safety Distance Limits for a Human near a Cellular Base Station Antenna, Adopting the IEEE Standard or ICNIRP Guidelines", *Bioelectromagnetics*, vol. 23, no. 6, pp. 429-443, 2002.
- [21] A. Christ, A. Klingenböck, T. Samaras, C. Goiceanu and N. Kuster, "The Dependence of Electromagnetic Far-Field Absorption on Body Tissue Composition in the Frequency Range from 300 MHz to 6 GHz", *IEEE Transactions on Microwave Theory and Techniques*, vol. 54, no. 5, pp. 2188-2195, 2006.
- [22] M. A. A. Karunaratna and I. J. Dayawansa, "Energy Absorption by the Human Body from RF and Microwave Emissions in Sri Lanka", *Sri Lankan Journal of Physics*, vol. 7, pp. 35-47, 2006.
- [23] A. Hirata, S. Kodera, J. Wang and O. Fujiwara, "Dominant Factors Influencing Whole-Body Average SAR Due to Far-Field Exposure in Whole-Body Resonance Frequency and GHz Regions", *Bioelectromagnetics*, vol. 28, no. 6, pp. 484-487, 2007.
- [24] A. Hirata, N. Ito, O. Fujiwara, T. Nagaoka and S. Watanabe, "Conservative Estimation of Whole-Body-Averaged SARs in Infants with a Homogeneous and Simple-Shaped Phantom in the GHz Region", *Physics in Medicine & Biology*, vol. 53, no. 24, pp. 7215-7223, 2008.
- [25] T. Iyama, T. Onishi, Y. Tarusawa, S. Uebayashi and T. Nojima, "Novel Specific Absorption Rate (SAR) Measurement Method Using a Flat Solid Phantom", *IEEE Transactions on Electromagnetic Compatibility*, vol. 50, no. 1, pp. 43-51, 2008.
- [26] L. Liu, N. K. Nikolova and N. T. Sangary, "Evaluation of the Specific Absorption Rate and the Temperature Rise in the Human Eyes with Account for Resonance", *IEEE Transactions on Microwave Theory and Techniques*, vol. 57, no. 12, pp. 3450-3460, 2009.
- [27] A. Y. Simba, T. Hikage, S. Watanabe and T. Nojima, "Specific Absorption Rates of Anatomically Realistic Human Models Exposed to RF Electromagnetic Fields From Mobile Phones Used in Elevators", *IEEE Transactions on Microwave Theory and Techniques*, vol. 57, no. 9, pp. 1250-1259, 2009.
- [28] T. Wessapan, S. Srisawatdhisukul and P. Rattanadecho, "Specific Absorption Rate and Temperature Distributions in Human Head Subjected to Mobile Phone Radiation at Different Frequencies", *International Journal of Heat and Mass Transfer*, vol. 55, no. 1-3, pp. 347-359, 2012.
- [29] T. Wessapan, P. Rattanadecho, "Specific Absorption Rate and Temperature Increase in the Human Eye due to Electromagnetic Fields Exposure at Different Frequencies", *International Journal of Heat and Mass Transfer*, vol. 64, pp. 426-435, 2013.
- [30] A. Kundu, "Specific Absorption Rate Evaluation in Apple Exposed to RF Radiation from GSM Mobile Towers", *IEEE Applied Electromagnetics Conference (AEMC) 2013*, pp. 1-2, India, 2013.
- [31] A. Kundu, *RF Energy Absorption in Plant Parts due to Cell Tower Radiation*, Germany, LAP Lambert Academic Publishing, 2015.
- [32] A. Kundu and B. Gupta, "Specific Absorption Rate Evaluation of Apple as per FCC RF Exposure Guideline", *Recent Development in Electrical, Electronics and Engineering Physics (RDE3P-2013)*, pp. 152-156, Kolkata, India, 2013.
- [33] A. Kundu and B. Gupta, "Comparative SAR Analysis of Some Indian Fruits as per the Revised RF Exposure Guideline", *IETE Journal of Research*, vol. 60, no. 4, pp. 296-302, 2014.
- [34] A. Kundu, B. Gupta and A. I. Mallick, "SAR Analysis in a Typical Bunch of Grapes Exposed to Radio Frequency Radiation in Indian Scenario", *IEEE International Conference on Microelectronics, Computing and Communication (MicroCom2016)*, pp. 1-5, India, 2016.
- [35] A. Kundu, B. Gupta and A. I. Mallick, "Specific Absorption Rate Evaluation in a Typical Multilayer Fruit: Coconut with Twig due to Electromagnetic Radiation as per Indian Standards", *Microwave Review (Mikrotalasana Revija)*, vol. 23, no. 2, pp. 24-32, 2017.
- [36] A. Kundu, B. Gupta and A. I. Mallick, "Dependence of Electromagnetic Energy Distribution inside a Typical Multilayer Fruit Model on Direction of Arrival and Polarization of Incident Field", *2019 IEEE Radio and Antenna Days of the Indian Ocean (RADIO)*, pp. 1-2, Reunion, 2019.
- [37] A. Kundu, B. Gupta and A. I. Mallick, "Contrast in Specific Absorption Rate for a Typical Plant Model due to Discrepancy Among Global and National Electromagnetic Standards", *Progress In Electromagnetics Research M*, vol. 99, pp. 139-152, 2021.
- [38] A. Kundu, B. Gupta and A. I. Mallick, "Dependence of Specific Absorption Rate and its Distribution inside a Homogeneous Fruit Model on Frequency, Angle of Incidence, and Wave Polarization", *Frequenz*, 2021. Available at: <https://doi.org/10.1515/freq-2021-0049>

- [39] R. F. Cleveland Jr., D. M. Sylvar and J. L. Ulcek, *Evaluating Compliance with FCC Guidelines for Human Exposure to Radio Frequency Electromagnetic Fields*, FCC OET Bulletin.65, Washington D.C., 1997.
- [40] International Commission on Non-Ionizing Radiation Protection (ICNIRP), “Guidelines for Limiting Exposure to Electromagnetic Fields (100 kHz to 300 GHz)”, *Health Physics*, vol. 118, no. 5, pp. 483-524, 2020.
- [41] Department of Telecommunications (DoT), *A Journey for EMF*, Department of Telecommunications website, Ministry of Communications, Govt. of India. <http://dot.gov.in/journey-emf>, Accessed 01 Jan 2020.
- [42] Swiss Agency for the Environment, Forests and Landscape (SAEFL), *Electrosmog in the Environment*, Federal Office for the Environment website. <https://www.bafu.admin.ch/bafu/en/home/topics/electrosmog/publications-studies/publications/electrosmog-in-the-environment.html>, 2005. Accessed 01 Jan 2020.
- [43] P. Vecchia, “Radiofrequency Fields: Bases for Exposure Limits”, *2 European IRPA Congress on Radiation Protection - Radiation Protection: From Knowledge to Action*, Paris, France, 2006.
- [44] H. Mazar, “A Global Survey and Comparison of Different Regulatory Approaches to Non-Ionizing RADHAZ and Spurious Emissions”, *IEEE International Conference on Microwaves, Communications, Antennas and Electronics Systems (COMCAS)*, pp. 1-6, Tel Aviv, 2009.
- [45] G. Kumar, *Report on Cell Tower Radiation*, submitted to secretary, Department of Telecommunications (DoT), Delhi, 2010. <https://www.ee.iitb.ac.in/~mwave/GK-cell-tower-rad-report-DOT-Dec2010.pdf>, 2010. Accessed 01 Jan 2020.
- [46] S. Lin-Liu and W. R. Adey, “Low Frequency Amplitude Modulated Microwave Fields Change Calcium Efflux Rates from Synaptosomes”, *Bioelectromagnetics*, vol. 3, no. 3, pp. 309-322, 1982.
- [47] S. Kwee and P. Raskmark, “Changes in Cell Proliferation due to Environmental Non-Ionizing Radiation: 2. Microwave Radiation”, *Bioelectrochemistry and Bioenergetics*, vol. 44, no. 2, pp. 251-255, 1998.
- [48] S. Velizarov, P. Raskmark and S. Kwee, “The Effects of Radiofrequency Fields on Cell Proliferation are Non-Thermal”, *Bioelectrochemistry and Bioenergetics*, vol. 48, no. 1, pp. 177-180, 1999.
- [49] E. A. Navarro, J. Segura, M. Portolés and C. Gómez-Perretta de Mateo, “The Microwave Syndrome: A Preliminary Study in Spain”, *Electromagnetic Biology and Medicine*, vol. 22, no. 2-3, pp. 161-169, 2003.
- [50] D. Remondini, R. Nylund, J. Reivinen, F. Pouletier de Gannes, B. Veyret, I. Lagroye, E. Haro, M. A. Trillo, M. Capri, C. Franceschi and K. Schlatterer, “Gene Expression Changes in Human Cells after Exposure to Mobile Phone Microwaves”, *Proteomics*, vol. 6, no. 17, pp. 4745-4754, 2006.
- [51] H. Hinrikus, M. Bachmann, D. Karai and J. Lass, “Mechanism of Low-Level Microwave Radiation Effect on Nervous System”, *Electromagnetic Biology and Medicine*, vol. 36, no. 2, pp. 202-212, 2017.
- [52] D. J. Panagopoulos, M. Cammaerts, D. Favre and A. Balmori, “Comments on Environmental Impact of Radiofrequency Fields from Mobile Phone Base Stations”, *Critical Reviews in Environmental Science and Technology*, vol. 46, no. 9, pp. 885-903, 2016.
- [53] S. Sivani and D. Sudarsanam, “Impacts of Radio-Frequency Electromagnetic Field (RF-EMF) from Cell Phone Towers and Wireless Devices on Biosystem and Ecosystem – A Review”, *Biology and Medicine*, vol. 4, no. 4, pp. 202-216, pp. 2012.
- [54] M. S. Venkatesh and G. S. V. Raghavan, “An Overview of Dielectric Properties Measuring Techniques”, *Canadian Biosystems Engineering*, vol. 47, no. 7, pp. 15-30, 2005.
- [55] A. P. Gregory and R. N. Clarke, “A Review of RF and Microwave Techniques for Dielectric Measurement on Polar Liquids”, *IEEE Transactions on Dielectrics and Electrical Insulation*, vol. 13, no. 4, pp. 727-743, 2006.
- [56] S. N. Jha, K. Narasaiah and A. L. Basediya, “Measurement Techniques and Application of Electrical Properties for Nondestructive Quality Evaluation of Foods – A Review”, *J Food Sci Technol.*, vol. 48, no. 4, pp. 387-411, 2011.
- [57] G. Deschamps, “Impedance of an Antenna in a Conducting Medium”, *IRE Transactions on Antennas and Propagation*, vol. 10, no. 5, pp. 648-650, 1962.
- [58] L. Liu, D. Xu and Z. Jiang, “Improvement in Dielectric Measurement Technique of Open-Ended Coaxial Line Resonator Method”, *Electronics Letters*, vol. 22, no. 7, pp. 373-375, 1986.
- [59] R. Zajíček, J. Vrba and K. Novotný, “Evaluation of a Reflection Method on an Open-Ended Coaxial Line and its Use in Dielectric Measurements”, *Acta Polytechnica*, vol. 46, no. 5, pp. 50-54, 2006.
- [60] R. Zajíček, L. Oppl and J. Vrba, “Broadband Measurement of Complex Permittivity Using Reflection Method and Coaxial Probes”, *Radioengineering*, vol. 17, no. 1, pp. 14-19, 2008.
- [61] D. M. Hagl, D. Popovic, S. C. Hagness, J. H. Booske and M. Okoniewski, “Sensing Volume of Open-Ended Coaxial Probes for Dielectric Characterization of Breast Tissue at Microwave Frequencies”, *IEEE Transactions on Microwave Theory and Techniques*, vol. 51, no. 4, pp. 1194-1206, 2003.
- [62] J. S. Bobowski and T. Johnson, “Permittivity Measurements of Biological Samples by an Open-Ended Coaxial Line”, *Progress in Electromagnetics Research B*, vol. 40, pp. 159-183, 2012.
- [63] CST STUDIO SUITE 2014. <https://www.3ds.com/products-services/simulia/products/cst-studio-suite/> Accessed 01 Jan 2020
- [64] Institute of Electrical and Electronics Engineers (IEEE), *IEEE Recommended Practice for Measurements and Computations of Radio Frequency Electromagnetic Fields with Respect to Human Exposure to Such Fields, 100 kHz-300 GHz*, IEEE Std C95.3-2002 (Revision of IEEE Std C95.3-1991), pp. 1-126, 2002. doi: 10.1109/IEEESTD.2002.94226
- [65] Institute of Electrical and Electronics Engineers (IEEE), *IEC/IEEE International Standard - Determining the Peak Spatial-Average Specific Absorption Rate (SAR) in the Human Body from Wireless Communications Devices, 30 MHz to 6 GHz - Part 1: General Requirements for Using the Finite-Difference Time-Domain (FDTD) Method for SAR Calculations*. IEC/IEEE 62704-1: 2017, pp. 1-86, 2017. doi: 10.1109/IEEESTD.2017.8088404
- [66] K. Bhattacharya, “On the Dependence of Charge Density on Surface Curvature of an Isolated Conductor”, *Physica Scripta*, vol. 91, no. 3, 035501, 2016.
- [67] E. C. Jordan and K. G. Balmain, *Electromagnetic Waves and Radiating Systems (2nd Edition)*, New Jersey, PHI, 2009.
- [68] M. D. Deshpande, C. R. Cockrell, F. B. Beck, E. Vedeler and M. B. Koch, “Analysis of Electromagnetic Scattering from Irregularly Shaped, Thin, Metallic Flat Plates”, *NASA Technical Paper 3361*, 1993.
- [69] D. Roux, A. Vian, S. Girard, P. Bonnet, F. Paladian, E. Davies and G. Ledoit, “Electromagnetic Fields (900 MHz) Evoke Consistent Molecular Responses in Tomato Plants”, *Physiologia Plantarum*, vol. 128, no. 2, pp. 283-288, 2006.
- [70] D. Roux, A. Vian, S. Girard, P. Bonnet, F. Paladian, E. Davies and G. Ledoit, “High Frequency (900 MHz) Low Amplitude (5 V m^{-1}) Electromagnetic Field: A Genuine Environmental Stimulus that Affects Transcription, Translation, Calcium and

- Energy Charge in Tomato”, *Planta*, vol. 227, no. 4, pp. 883-891, 2008.
- [71] D. Roux, C. Faure, P. Bonnet, S. Girard, G. Ledoigt, E. Davies, M. Gendraud, F. Paladian and A. Vian, “A Possible Role for Extra-Cellular ATP in Plant Responses to High Frequency, Low Amplitude Electromagnetic Field”, *Plant Signaling & Behavior*, vol. 3, no. 6, pp. 383-385, 2008.
- [72] A. Vian, E. Davies, M. Gendraud and P. Bonnet, “Plant Responses to High Frequency Electromagnetic Fields”, *BioMed Research International*, vol. 2016, article no. 1830262, pp. 1-13, 2016.
- [73] A. Kundu, S. Vangaru, S. Bhattacharyya, A. I. Mallick and B. Gupta, “Electromagnetic Irradiation Evokes Physiological and Molecular Alterations in Rice”, *Bioelectromagnetics*, vol. 42, no. 2, pp. 173-185, 2021.
- [74] A. Kundu, S. Vangaru, S. Bhattacharyya, A. I. Mallick and B. Gupta, “Erratum: Electromagnetic Irradiation Evokes Physiological and Molecular Alterations in Rice”, *Bioelectromagnetics*, vol. 42, no. 5, pp. 435-435, 2021.
- [75] A. Kundu, S. Vangaru, S. Bhowmick, S. Bhattacharyya, A. I. Mallick and B. Gupta, “One-time Electromagnetic Irradiation Modifies Stress-sensitive Gene Expressions in Rice Plant”, *Bioelectromagnetics*, vol. 42, no. 8, pp. 649-658, 2021.